Flexural behaviour of lightly cement stabilized materials: South Africa and Brazil

William Fedrigo[a,*], Alex T. Visser[b], Wynand JvdM Steyn[b] and Washington Peres Núñez[a]

[a]Department of Civil Engineering, Federal University of Rio Grande do Sul, Porto Alegre, Brazil;

[b]Department of Civil Engineering, University of Pretoria, Pretoria, South Africa

*Corresponding author. Email: william.fedrigo@ufrgs.br

This paper focuses on the flexural behaviour of lightly cement stabilized materials. An experimental programme was developed to analyse the effects of compaction method, test setup and displacement rate on the static behaviour, to characterize the laboratory fatigue behaviour of South African materials and to compare South African and Brazilian materials. Similar flexural properties were achieved using vibration and compression compaction methods. The South African setup leads to lower strength and stiffness values, but to a better prediction of the field modulus. The static properties are not affected by the displacement rate. The strain at break is not affected by any tested variable, being the most meaningful property for design. Strain-based models provide a better fatigue life prediction than the stress-based models. Laboratory models lead to a fatigue life shorter than the South African field transfer functions. Similarities were observed between South African and Brazilian materials, which suggests comparable fatigue performances.

Keywords: lightly cement stabilized material; flexural behaviour; strain at break; fatigue; South Africa; Brazil

1 Introduction

Lightly cement stabilised materials (LCSM) are being increasingly used in the construction and rehabilitation of pavements due to the increase in traffic demand and load (Sounthararajah et al., 2017). These materials are the product of soil stabilization with cementitious binders (e.g. cement and lime) that outperform granular materials and undergo fatigue when subjected to traffic loading. Thus, fatigue is the main design criteria for long-term performance of cement stabilized layers (Jitsangiam et al., 2016).

The four-point bending test (4PBT) is often used to characterize the behaviour and to obtain design parameters of LCSM. The test measures the stress states to which stabilized layers are subjected, such as the development of tensile and compressive stresses at the bottom and top of the beam, respectively (Fu et al., 2009). Although

researchers have investigated the flexural behaviour of LCSM since the 1970s (Otte, 1972; Otte, 1978; Pretorius, 1970), no universal test method was established. The method used to perform the tests can affect the results and consequently the pavement design. For instance, results obtained in South Africa may greatly differ from those obtained in Brazil, even if the same materials are tested.

In this regard, a literature review of previous studies showed that the main differences between flexural test methods for LCSM are: (a) the compaction method used to produce the beams; (b) the test setup (i.e. beam section and span between support rollers); and (c) the static test mode (i.e. under load, stress or displacement control) and the rate of load application (speed). Furthermore, no laboratory fatigue characterization of South African materials was found in the literature. The South African fatigue models were based on accelerated pavement testing (APT), while most of the fatigue models used worldwide (e.g. Brazil) were developed essentially based on flexural cyclic tests.

Considering the mentioned differences between the test methods for flexural characterization of LCSM used in South Africa and internationally, especially in Brazil, the objectives of the research reported were: (a) to analyse and quantify the effects of compaction method, test setup and displacement rate on the flexural static behaviour; (b) to characterize the laboratory fatigue behaviour of South African LCSM; and (c) to compare the flexural behaviour of South African and Brazilian LCSM.

2 Literature review

2.1 Compaction method

Several compaction methods to produce specimens for flexural tests are reported in the literature. In South Africa, vibratory table compaction in conjunction with surcharges

placed over the material was used in the past (Otte, 1972; Otte, 1978). This method was based on the work by Pretorius (1970) and the same kind of compaction method was recently used by other authors (Linares-Unamunzaga et al., 2018), although vibrating hammers are preferred nowadays (Farhan et al., 2019; Farhan et al., 2015; Katsakou & Kolias, 2007; Kolias, 1996a; Kolias, 1996b; Kolias et al., 2001; Mbaraga et al., 2014). In a way similar to what is done in the United States (Mandal et al., 2018; Mandal et al., 2016; National Cooperative Highway Research Program, NCHRP, 2014) and elsewhere (Biswal et al., 2018a; Biswal et al., 2018b; Thichês, 1993), some South African researchers also used the modified AASHTO hammer (Liebenberg, 2002; Liebenberg, 2003; Liebenberg & Visser, 2003; Liebenberg & Visser, 2004; Mgangira, 2011; Robroch, 2002) and even a protocol was developed (Council for Scientific and Industrial Research, CSIR, 2011). In Brazil, beams are produced by means of press compression (Castañeda López et al., 2018; Fedrigo et al., 2018; Nascimento & Albuquerque, 2018, Paiva et al., 2017), mainly based on the Australian experience (Arulrajah et al., 2015; Disfani et al., 2014; González et al., 2013).

No study regarding the effect of the compaction method on the flexural behaviour of LCSM was found in the literature. However, Otte (1972) reported that beams produced using vibratory table compaction have the same density as those produced using press compaction but are more homogeneous and stiffer (ultrasonic test). The author then suggested that vibratory compaction is more representative of field compaction. This statement was confirmed by other authors, although based only on unconfined compressive strength (UCS) tests (Ji et al., 2018; Jiang & Fan, 2013).

2.2 Test setup

Most commonly a 100 mm × 100 mm section beam and a 300 mm span between support rollers was used for the test setup (Farhan et al., 2019; Farhan et al., 2015; Jia et

al., 2018; Katsakou & Kolias, 2007; Kolias, 1996a; Kolias, 1996b; Kolias et al., 2001; Xiao et al., 2017). Recent Brazilian studies used the same test setup (Castañeda López et al., 2018; Fedrigo et al., 2018; Nascimento & Albuquerque, 2018; Paiva et al. 2017) in accordance with the Australia and United States experience (Arulrajah et al., 2015; Austroads, 2008; Disfani et al., 2014; González et al., 2013; Litwinowicz & Brandon, 1994; Mandal et al., 2018; Mandal et al., 2016; NCHRP, 2014). On the other hand, the South African setup differs from the rest of the world, using a 75 mm × 75 mm section beam and a span of 420 mm (CSIR, 2011; Liebenberg, 2002; Liebenberg, 2003; Liebenberg & Visser, 2003; Liebenberg & Visser, 2004; Mgangira, 2011; Otte, 1972; Otte, 1978; Robroch, 2002). Its development was based on the following (Otte, 1972): (a) the ratio of span to depth (height) must not be less than 5; (b) the ratio of the minimum beam dimension to the maximum aggregate size should exceed 3; and (c) reduction of the influence of shear force on the deflection.

Mbaraga et al. (2014) reported that flexural strength and stiffness increase with the use of wide spans and small heights, as well as if smaller aggregates are used as the maximum particle size. This agrees with the statements made by Otte (1972), although the South African setup was not compared with others reported elsewhere. It is worth emphasizing that tests using 75 mm × 75 mm (3 inches × 3 inches) section beams were reported elsewhere, including in Brazil, but in conjunction with different spans (Biswal et al., 2018a; Biswal et al., 2018b; Ceratti, 1991; Gnanendran & Paul, 2016; Paul & Gnanendran, 2012; Paul & Gnanendran, 2015; Paul et al., 2015; Pretorius, 1970).

2.3 Test mode and rate of application

The flexural static test mode (i.e. under load, stress or displacement control) and the rate of load application (speed) also differ from one region to another. South African studies were performed using displacement control and the displacement rates varied from 1.0

to 1.8 mm/min (CSIR, 2011; Liebenberg, 2002; Liebenberg, 2003; Liebenberg & Visser, 2003; Liebenberg & Visser, 2004; Mbaraga et al., 2014; Mgangira, 2011; Otte, 1972; Otte, 1978; Robroch, 2002). In the rest of the world, tests are often performed using load or stress control (Arulrajah et al., 2015; Austroads, 2008; Ceratti, 1991; Disfani et al., 2014; González et al., 2013; Jitsangiam et al., 2016; Katsakou & Kolias, 2007; Kolias, 1996a; Kolias, 1996b; Kolias et al., 2001; Linares-Unamunzaga et al., 2018; Nascimento & Albuquerque, 2018; Paiva et al., 2017; Pretorius, 1970; Sounthararajah et al., 2018; Sounthararajah et al., 2017; Sounthararajah et al., 2016), although a few authors used displacement control (Farhan et al., 2019; Farhan et al., 2015; Gnanendran & Paul, 2016; Paul & Gnanendran, 2012; Paul & Gnanendran, 2015; Paul et al., 2015).

In Brazil, the tests are performed under stress control by applying a rate of 0.69 MPa/min (Castañeda López et al., 2018; Fedrigo et al., 2018), in accordance with the United States experience (Mandal et al., 2018; Mandal et al., 2016; NCHRP, 2014). Paul & Gnanendran (2012) reported that the stress rate of 0.69 MPa/min is equivalent to a displacement rate of 0.5 mm/min. The authors also verified that the flexural strength and stiffness increase with increases in the displacement rate, although they had not tested the rates used in South Africa.

2.4 Cyclic tests

There are also differences related only to the flexural cyclic (or fatigue) tests. A literature survey of the above-mentioned studies showed that generally the factors that vary most are the applied loading frequency and stress levels. Moreover, the tests are often carried out in a stress-controlled mode, applying a haversine load pulse and terminated when the specimen fails. Note that no laboratory fatigue characterization of South African LCSM was found in the literature. The fatigue transfer functions included

in the South African mechanistic pavement design method (South African National Roads Agency Limited, SANRAL, 2014; Theyse et al., 1996) are based on the extensive data collected and analysed by Otte (1972; 1978) and De Beer (1985; 1990) using APT. On the other hand, most of the fatigue models used internationally, including in Brazil, were developed based on laboratory results.

3 Experimental programme

The study can be divided into three stages, in accordance with the defined study objectives. In the first stage, the flexural static characterization (modulus of rupture, strain at break and stiffness) of the studied LCSM was carried out in specimens produced with three compaction methods (vibratory table, press and hammer), using two test setups (100 mm × 100 mm × 300 mm and 75 mm × 75 mm × 420 mm) and applying three displacement rates (0.5, 1.0 and 1.8 mm/min). The effect of the independent variables was individually evaluated at this stage (a detailed description is provided in Table 3, Section 3.3.1). The second stage comprised the flexural cyclic characterization (modulus, degradation, fatigue life) of the studied materials. In the third and final stage, the flexural static and cyclic behaviour of the studied South African materials was compared to that of Brazilian materials. The testing conditions used in the first and second stages were selected in order to allow these comparisons. The experimental programme is described in detail in the following sections, including the mechanistic pavement analysis done in this study.

3.1 Materials

Two natural gravels (G6 materials) were stabilized for the laboratory tests. Table 1 and Figure 1 show their characteristics and grain size distributions, respectively. The weathered granite was obtained from a quarry located near Johannesburg. The burnt

shale was used as parent material to produce the LCSM base layer of an experimental section located on the R104 road near Pretoria. This material was collected from the shoulder of the mentioned road, where it was used without stabilization.

Table 1

Figure 1

Mix designs to obtain C3 materials (UCS between 1.5 and 3 MPa) were performed by evaluating the initial consumption of stabilizer (ICS), UCS and indirect tensile strength (ITS). The granite was tested using 2.5%, 3.5% and 4.5% of portland cement with fly ash and slag addition and strength class of 32.5 MPa (RoadCem CEM II/B-M (V-S) 32.5 N). To reduce its Plasticity Index, the shale was pre-treated with 1% of hydrated lime (Calcitic Road Lime) and then tested with 1%, 2% and 3% of the same cement as that used to stabilize the granite. Table 2 shows the resulting mix design characteristics. The shale characterization and its mix design were done by Theyse (2013). The UCS of both materials achieved values higher than 3 MPa, but they were still considered C3 as the materials were G6 (Paige-Green, 2014).

Table 2

3.2 Specimens

Beams with sections of 100 mm × 100 mm (500 mm long) and 75 mm × 75 mm (450 mm long) were prepared. For the granite, solids were mixed and water at OMC was added while continuing mixing. For the shale, lime and water were added and mixed 24 hours prior to adding and mixing cement (Theyse, 2013). The material was compacted in three equal layers to achieve 97% MDD (CSRA, 1985) using one of the following methods: (a) vibratory table in conjunction with surcharges of approximately 50 kg (Figure 2(a)); (b) compression with a hydraulic press (Figure 2(b)); and (c) modified AASHTO hammer (56 blows per layer). To improve the bond between layers, their

surface was scarified. The specimens were wrapped in plastic sheets (Figure 2(c)) and cured at a temperature of 25 ºC for 28 days.

Figure 2

To reduce variability, specimens were discarded and remoulded when the following requirements were not met: (a) dry density lower than 97% of the MDD; and (b) effective moulding moisture content deviating by more than 1% of the OMC. A total of 30 beams with a section of 100 mm × 100 mm (21 from granite and 9 from shale) and 12 beams with a section of 75 mm × 75 mm (9 from granite and 3 from shale) were produced. Slabs were also taken from the shale LCSM of the R104 road experimental section (Figure 3(a)) and 6 beams with an age of 5.5 years (3 of each size) were sawed (Figure 3(b)).

Figure 3

3.3 Testing procedures

A hydraulic press with a capacity of 250 kN was used for static and cyclic tests. The actuator was controlled using a 20 kN load cell. 4PBT was used and the mid-span deflection was measured using two linear variable differential transducers (LVDTs).

3.3.1 Static tests

Flexural static tests were carried out in a displacement-controlled mode to evaluate the effects of the compaction method, test setup (Figure 4) and displacement rate on modulus of rupture (MOR, also known as flexural strength), strain at break (strain corresponding to MOR), stiffness and UCS (using cubes sawed from the tested beams). Eq. (1) was used to calculate the flexural stress. The flexural tensile strain was calculated using Eq. (2). The flexural static modulus (stiffness) was determined from the stress-strain relationships (secant modulus corresponding to 40% of MOR).

$$\sigma_i = \frac{P_i * L}{w * h^2} \quad (1)$$

$$\varepsilon_i = \frac{108 * h * \delta_i * 10^6}{23 * L^2} \quad (2)$$

Where σ_i (MPa) is the stress corresponding to force P_i (N); ε_i ($\mu\varepsilon$) is the tensile strain corresponding to the average deflection δ_i (mm); L is the length between supporting rollers, and; w and h are the average width and height (mm), respectively.

Figure 4

The effect of each independent variable was evaluated individually using Analysis of Variance (one-way ANOVA) while the levels of the remaining two were kept constant (Table 3). The variables and their levels were defined based on the literature review (Section 2). Three specimens were tested for each condition. The length between the loading rollers was equal to 1/3 of the span between supporting rollers.

Table 3

3.3.2 Cyclic tests

Flexural cyclic (fatigue) tests were carried out in a stress-controlled mode. Specimens were subjected to 3 Hz haversine cyclic loading (equipment maximum allowable frequency). A preload of 0.1 kN was maintained during the tests. The applied stress levels were 70%, 80% and 90% of the MOR. The tests were terminated after the failure of the specimens. Initial cyclic (resilient) modulus and initial strain were determined for the first load pulse because some specimens failed after only a few cycles. Some beams failed during the preload stage and no data was collected (ideally more sensitive equipment was needed).

The test characteristics were defined to allow comparisons with Brazilian materials. The vibratory table compaction was used since it was the easiest way to produce the beams and due to the reasons reported in Section 4.1. The 100 mm × 100 mm × 300 mm setup was used. The MOR used to determine the stress levels was the average obtained using a displacement rate of 0.5 mm/min since it is equivalent to the stress rate of 0.69 MPa/min (Paul & Gnanendran, 2012) and due to the reasons reported in Section 4.3.

3.4 Mechanistic pavement analysis

In order to compare field and laboratory modulus values, the modulus of the pavement layers of the R104 road experimental section was back-calculated using the Falling Weight Deflectometer (FWD) data collected by Theyse (2013) 28 days after construction. GAMES software (Maina & Matsui, 2004) was used to run the analysis. A structure consisting of 100 mm of C3 (observed when collecting the cement stabilized shale slabs), 400 mm of G7 (100 mm of neat G6 plus 300 mm of selected G7) and G7 subgrade was considered. The respective Poisson's ratios were 0.25, 0.35 and 0.44.

A mechanistic pavement analysis was also performed to compare the results obtained using the cement stabilized shale strain-based fatigue model and the South African transfer functions. Everstress software (Washington State Department of Transportation, WSDOT, 2005) was used to run the analysis. The structure of the R104 road experimental section was used in the analysis. The properties considered for the stabilized shale were those obtained in this study and those historically used in South Africa. Two 20 kN wheel loads and tire pressures of 560 kPa and 800 kPa were considered.

4 Static tests results

According to the detailed programme shown in Table 3, the following sections present the effects of compaction method, test setup and displacement rate in the static tests results.

4.1 Effect of the compaction method

Figure 5 shows the stress-strain relationships for the individual beams. Figure 6 shows the flexural static properties as a function of the compaction method. The values are the average of three specimens and the error bars represent the standard deviation (SD). The highest values of MOR (Figure 6(a)), UCS (Figure 6(b)) and modulus (Figure 6(d)) as well as the lowest value of strain at break (Figure 6(c)) were obtained using vibratory table compaction, which is followed by the press compaction and then by the hammer compaction. The obtained values of strain at break and modulus were higher than those recommended in South Africa for the design of C3 layers (SANRAL, 2014; Theyse et al., 1996). The UCS values obtained for the beams compacted using vibratory table were higher than those suggested for C3 materials (CSRA, 1985; Theyse et al., 1996).

Figure 5

Figure 6

Table 4 shows the results of the One-Way ANOVA (significance level of 0.05). A multiple comparison of means was also performed (Tukey's test) and groups were defined. Means that do not share a group letter are significantly different. The effect of the compaction method on strain at break and modulus was not significant. The compaction method effect on the MOR was significant but there was no difference between the means obtained using vibratory table and press. The highest effect due to

the compaction method was on the UCS, which allows the deduction that the compression behaviour is more affected by the compaction than the tensile behaviour.

Table 4

4.2 Effect of the test setup

Figure 7 shows the stress-strain relationships of the specimens of granite (28 days) and shale (28 days and 5.5 years) obtained using the two test setups. Figure 8 shows the flexural static properties as a function of the test setup for the two materials. The shale was stronger and stiffer than the granite, possibly due to the lower ICS value and the higher amount of stabilizer. The average values of all properties decreased with the use of the 75 mm × 75 mm × 420 mm setup. The opposite trend was reported by Mbaraga et al. (2014). However, this could be an effect of the interaction between maximum aggregate size and beam section instead of an effect of the setup itself since larger aggregates can generate weak spots in a smaller specimen.

Figure 7

Figure 8

The effect of the curing time can be observed since all properties of the shale increased with age. The obtained values of strain at break (Figure 8(c)) were higher than suggested for the design of C3 layers (SANRAL, 2014; Theyse et al., 1996). The same was observed for the UCS values (Figure 8(b)). Furthermore, other authors reported that the UCS of concrete increases as the cube size decreases (Leung & Ho, 1996; Van Schalkwyk & Kearsley, 2018; Yi et al., 2006). Although the mentioned authors have not used 75 mm cubes, this was also observed for the shale after 5.5 years. On the other hand, the UCS of both materials after 28 days decreased with the decrease in cube size. This fact was also reported by Tokyay & Özdemir (1997) for concrete cubes of the

same sizes and age as those used in this study. All these facts show that no correction factor can be suggested.

The modulus values (Figure 8(d)) obtained using the 75 mm × 75 mm × 420 mm setup were the closest to the recommended for design (SANRAL, 2014; Theyse et al., 1996). The back-calculated moduli for the C3 base (cement stabilized shale), G7 subbase and G7 subgrade were 1331 MPa (SD = 639 MPa), 241 MPa (SD = 95 MPa) and 167 MPa (SD = 36 MPa), respectively. The modulus obtained using the 75 mm × 75 mm × 420 mm setup (2908 MPa) was the closest to the field one (1331 MPa), although being more than twice the latter.

The results of One-Way ANOVA and comparison of means are presented in Table 5. Regardless of the material or age, the test setup effect on MOR and modulus was significant and there were significant differences between the means. On the other hand, the effect of the test setup on strain at break and UCS (75 mm cubes versus 100 mm cubes) was not statistically significant (although there were differences between the average values of UCS as shown in the comments presented above).

Table 5

4.3 Effect of the displacement rate

The stress-strain relationships of the specimens are presented in Figure 9. Figure 10 shows the static properties as a function of the displacement rate. The average values of MOR (Figure 10(a)) and modulus (Figure 10(d)) increased and the strain at break (Figure 10(c)) decreased with an increase in the displacement rate, which was also reported by Paul & Gnanendran (2012). There were no evident changes in the UCS as the regions from where cubes were cut are not affected by the loading. The average values of strain at break and UCS were higher than the suggested for C3 layers design. The average modulus obtained for a displacement rate of 0.5 mm/min was close to the

recommended for the design of C3 layers (CSRA, 1985; SANRAL, 2014; Theyse et al., 1996), which suggests that this rate might be the most adequate.

Figure 9

Figure 10

The results of One-Way ANOVA and comparison of means are presented in Table 6. Regardless of the tested property, there were no significant effects and all the means were categorized into the same group. Therefore, for the tested levels, the displacement rate does not have a statistical effect on the flexural static behaviour.

Table 6

5 Cyclic tests results

The cyclic (fatigue) tests results are summarized in Table 7 and are analysed in the next sections. No statistical analysis was made due to the limited number of specimens.

Table 7

5.1 Cyclic (resilient) modulus

Figure 11 shows a comparison between the moduli obtained for both materials. The average cyclic (resilient) modulus values (considering all specimens) were comparable to the static modulus values. This suggests that static tests could be used to determine the design modulus since they are easier to undertake than the cyclic tests. Castañeda López et al. (2018) reported similar trends for Brazilian materials. For the shale (Figure 11(b)), the laboratory moduli were four times higher than the field modulus.

Figure 11

5.2 Degradation

Figure 12 shows the degradation of the specimens in terms of normalized modulus

(ratio of the modulus at any load cycle to the initial modulus) against normalized number of cycles (ratio of any number of cycles to the number of cycles at failure). The typical pattern of LCSM showing three damage phases (González et al., 2013; Jia et al., 2018; Mandal et al., 2018; Mandal et al., 2016) was only observed for specimens subjected to the lower stress level (70%). For the others, the stiffness reduced according to a slow and nearly constant rate from the beginning until the end of the test. Most specimens failed when their stiffness reached approximately 50% of the initial stiffness.

Figure 12

5.3 Fatigue models

Figure 13 shows the fatigue models obtained for the granite and shale. The figure shows similar models for both materials. The strain-based models (Figure 13(a)) provide a better prediction of the fatigue life than the stress-based models (Figure 13(b)), as the variability is less (coefficient of determination, R^2, and standard error of estimate, SEE). Pretorius (1970) observed similar trends for soil-cement. Figure 13(a) shows that the laboratory models lead to a fatigue life shorter than the South African transfer functions (TF) (SANRAL, 2014; Theyse et al., 1996), regardless of the reliability level (RL). The maximum allowable strain for the laboratory models is approximately half of the strain at break, while it can be much higher for the transfer functions. These facts indicate that the laboratory tests are more destructive than the field tests (APT), possibly because in the field the LCSM is part of a structure and it is supported by another layer.

Figure 13

5.4 Mechanistic pavement analysis results

Table 8 shows that the laboratory model obtained for the cement stabilized shale resulted in only one load repetition for all the analysed conditions. The number of load

repetitions obtained using the transfer functions decreased with the South African historic parameters and with the increase of tire pressure and RL. The difference between laboratory and field results ranged from 10^4 to 10^6 load repetitions, confirming the comments of Section 5.3.

Table 8

6 Comparison between South African and Brazilian materials

In the past, several Brazilian researchers studied the mechanical and fatigue behaviour of cement stabilized materials (Balbo, 1993; Ceratti, 1991; Trichês, 1993). However, the use of this kind of material still is limited in Brazil. Use is increasing because full-depth reclamation with cement is becoming a popular pavement rehabilitation technique. In this regard, two Brazilian materials (Fedrigo et al., 2017; Castañeda López et al., 2018) were selected according to the 7-day UCS range for C3 (CSRA, 1985; Theyse et al., 1996). These materials are cement stabilized (2%) mixtures of aggregates (80% and 50%) and reclaimed asphalt pavement, RAP (20% and 50%). The strain at break values and the fatigue models were re-evaluated since the mentioned authors used a different approach as the one used in this study to analyse them. For the South African materials, the used properties were those obtained using the test characteristics mentioned in Section 3.3.2.

Figure 14 shows the properties of the South African and Brazilian materials and the statistics are presented in Table 9. No statistical analysis was made for the cyclic (resilient) modulus due to the different number of specimens tested. The effect of the material was significant for all analysed properties, but some means were not significantly different (Tukey's test). The shale and the 20% RAP mixture were categorized into the same groups for strain at break (group B) and static modulus (group A), two of the main design parameters. This fact associated with the similarity between

their fatigue models (Figure 15) could suggest that a South African cement stabilized shale and a Brazilian cement stabilized recycled material with up to 20% RAP would have comparable fatigue performances. It is not possible to only compare the fatigue behaviour of different materials by observing their fatigue models since they might have different strength and stiffness.

Figure 14

Table 9

Figure 15

7 Conclusions

The following are conclusions based on the data analysed in this paper (they may be only valid for the materials used in this research and for similar materials):

- Statistically, similar flexural properties are obtained using vibratory table and press compaction methods. The compressive behaviour is more affected by the compaction method than the tensile behaviour. Considering the laboratory results, vibratory rollers are indicated for the compaction of lightly cement stabilized layers.
- The South African setup leads to lower flexural strength and stiffness values. However, this can be an effect of the interaction between maximum aggregate size and beam section instead of the setup itself. This setup also leads to a modulus value that is closer to the observed in the field, although the laboratory value is still much higher.
- The flexural static properties are not statistically affected by the testing displacement rate.

- The strain at break is not statistically affected by compaction method, setup and displacement rate. Therefore, it is the most adequate property for design.
- The average cyclic (resilient) modulus is similar to the average static modulus. Therefore, static tests could be used to determine the design modulus. This fact is important for practical use since static tests are more common and cheaper to execute than cyclic tests.
- The strain-based models provide a better prediction of the fatigue life than the stress-based models.
- The laboratory models lead to a fatigue life shorter than the South African transfer functions. A mechanistic pavement analysis confirmed this fact, showing a difference in the results ranging from 10^4 to 10^6 load repetitions.
- Statistics revealed similarities between the strain at break and modulus (two main design parameters) of a South African cement stabilized shale and a Brazilian cement stabilized recycled material. Their laboratory fatigue behaviours were also similar. These facts indicate that the mentioned materials could have comparable performances.

References

American Association of State Highway and Transportation Officials (AASHTO). (2010). Standard Method of Test for Moisture-Density Relations of Soils Using a 4.54-kg (10-lb) Rammer and a 457-mm (18-in.) Drop: AASHTO T 180-01, Washington, DC.

Arulrajah, A., Disfani, M. M., Haghighi, H., Mohammadinia, A., & Horpibulsuk, S. (2015). Modulus of rupture evaluation of cement stabilized recycled glass/recycled concrete aggregate blends. Construction and Building Materials, 84, 146–155.

Austroads. (2008). The development and evaluation of protocols for the laboratory characterisation of cemented materials, AP-T251-13. Sydney, Australia.

Balbo, J. T. (1993). Estudo das propriedades mecânicas das misturas de brita e cimento e sua aplicação aos pavimentos semi-rígidos [Study on the mechanical properties of mixtures of crushed rock and cement and theirs application in semirigid pavements] (Doctoral thesis). University of São Paulo, Brazil.

Biswal, D. R., Sahoo, U. C., & Dash, S. R. (2018a). Non-destructive strength and stiffness evaluation of cement-stabilised granular lateritic soils, Road Materials and Pavement Design.

Biswal, D. R., Sahoo, U. C., & Dash, S. R. (2018b). Mechanical characteristics of cement stabilised granular lateritic soils for use as structural layer of pavement, Road Materials and Pavement Design.

Castañeda López, M. A., Fedrigo, W., Kleinert, T. R., Matuella, M. F., Núñez, W. P., & Ceratti, J. A. P. (2018). Flexural fatigue evaluation of cement-treated mixtures of reclaimed asphalt pavement and crushed aggregates. Construction and Building Materials, 158, 320–325.

Ceratti, J. A. P. (1991). Estudo do comportamento a fadiga de solos estabilizados com cimento para utilização em pavimentos [Study on the fatigue behaviour of cement stabilized soils for pavements] (Doctoral thesis). Federal University of Rio de Janeiro, Brazil.

Committee of State Road Authorities (CSRA). (1985). Guidelines for road construction materials, Technical recommendations for highways: TRH 14. Pretoria, South Africa.

Committee of State Road Authorities (CSRA). (1986). Cementitious stabilizers in road construction, Technical recommendations for highways: TRH 13. Pretoria, South Africa.

Council for Scientific and Industrial Research (CSIR). (2011). Proposed Test Protocol for Stabilized Materials: Maximum Strain-at-Break Beam Test: Draft Version 1.0, Report SAPDM-B1C-2011-02. Pretoria, South Africa.

De Beer, M. (1985). Behaviour of cementitious subbase layers in bitumen base structures (Master's thesis). University of Pretoria, South Africa.

De Beer, M. (1990). Aspects of the design and behaviour of road structures incorporating lightly cementitious layers (Doctoral dissertation). University of Pretoria, South Africa.

Disfani, M. M., Arulrajah, A., Haghighi, H., Mohammadinia, A., & Horpibulsuk, S. (2014). Flexural beam fatigue strength evaluation of crushed brick as a

supplementary material in cement stabilized recycled concrete aggregates. Construction and Building Materials, 68, 667–676.

Farhan, A. H., Dawson, A. R., & Thom, N. H. (2019). Behaviour of rubberised cement-bound aggregate mixtures containing different stabilisation levels under static and cyclic flexural loading. Road Materials and Pavement Design.

Farhan, A. H., Dawson, A. R., Thom, N. H., Adam, S., & Smith, M. J. (2015). Flexural characteristics of rubberized cement-stabilized crushed aggregate for pavement structure. Materials and Design, 88, 897–905.

Fedrigo, W., Núñez, W. P., Castañeda López, M. A., Kleinert, T. R., & Ceratti, J. A. P. (2018). A study on the resilient modulus of cement-treated mixtures of RAP and aggregates using indirect tensile, triaxial and flexural tests. Construction and Building Materials, 171, 161–169.

Fedrigo, W., Núñez, W. P., Kleinert, T. R., Matuella, M. F., & Ceratti, J. A. P. (2017). Strength, shrinkage, erodibility and capillary flow characteristics of cement-treated recycled pavement materials. International Journal of Pavement Research and Technology, 10(5), 393–402.

Fu, P., Jones, D., Harvey, J. T., & Bukhari, S. A. (2009). Laboratory Test Methods for Foamed Asphalt Mix Resilient Modulus. Road Materials and Pavement Design, 10(1), 187–212.

Gnanendran, C. T., & Paul, D. K. (2016). Fatigue characterization of lightly cementitiously stabilized granular base materials using flexural testing. Journal of Materials in Civil Engineering, 28(9).

González, A, Jameson, G., Carteret, R., & Yeo, R. (2013). Laboratory fatigue life of cemented materials in Australia. Road Materials and Pavement Design, 14(3), 518–536.

Ji, X., Hou, Y., Li, X., & Wang, T. (2018). Comparison on properties of cement-stabilised gravel prepared by different laboratory compaction methods. Road Materials and Pavement Design.

Jia, Y., Liu, G., Gao, Y., Pei, J., Zhao, Y., & Zhang, J. (2018). Degradation reliability modeling of stabilized base course materials based on a modulus decrement process. Construction and Building Materials, 177, 303–313.

Jiang, Y. J., & Fan, L. F. (2013). An investigation of mechanical behavior of cement-stabilized crushed rock material using different compaction methods. Construction and Building Materials, 48, 508–515.

Jitsangiam, P., Nusit, K., Chummuneerat, S., Chindaprasirt, P., & Pichayapan, P. (2016). Fatigue assessment of cement-treated base for roads: An examination of beam-fatigue tests. Journal of Materials in Civil Engineering, 28(10), 1–11.

Katsakou, M., & Kolias, S. (2007). Mechanical properties of cement-bound recycled pavements. Proceedings of the Institution of Civil Engineers - Construction Materials, 160(4), 171–179.

Kolias, S. (1996a). Mechanical properties of cement-treated mixtures of milled bituminous concrete and crushed aggregates. Materials and Structures, 29, 411–417.

Kolias, S. (1996b). The influence of the type of loading and temperature on the modulus of elasticity of cement-bound mixes of milled bituminous concrete and crushed aggregates. Materials and Structures, 29, 543–551.

Kolias, S., Katsakou, M., & Kaloidas, V. (2001). Mechanical properties of flexible pavement materials recycled with cement. Proceedings of the 1st International Symposium on Subgrade Stabilization and In Situ Pavement Recycling Using Cement, Salamanca.

Leung, W. C., & Ho, K. S. (1996). Report on strength comparison of 100 mm and 150 mm cubes: Special Project Report SPR 3/96, Public Works Central Laboratory. Hong Kong.

Liebenberg, J. J. E. (2002). The Influence of Various Emulsion and Cement Contents on an Emulsion Treated Ferricrete from the HVS Test Sections on Road P243/1, Council for Scientific and Industrial Research (CSIR) Confidential Contract Report CR-2001/77. Pretoria, South Africa.

Liebenberg, J. J. E. (2003). A structural design procedure for emulsion treated pavement layers (Master's thesis). University of Pretoria, South Africa.

Liebenberg, J. J. E., & Visser, A. T. (2003). Stabilization and Structural Design of Marginal Materials for Use in Low-Volume Roads. Transportation Research Record, 1819, 166–172.

Liebenberg, J. J. E., & Visser, A. T. (2004). Stabilization and Structural Design of Marginal Materials for Use in Low-Volume Roads. Journal of the South African Institution of Civil Engineering, 46(3), 2–8.

Linares-Unamunzaga, A., Gonzalo-Orden, H., Minguela, J. D., & Pérez-Acebo, H. (2018). New Procedure for Compacting Prismatic Specimens of Cement-Treated Base Materials. Applied Sciences, 8(6), 970.

Litwinowicz, A., & Brandon, A. N. (1994). Dynamic flexure testing for prediction of cement-treated pavement life. Proceedings of the 17th Australian Road Research Board Conference, Gold Coast.

Maina, J. W., & Matsui, K. (2004). Developing Software for Elastic Analysis of Pavement Structure Responses to Vertical and Horizontal Surface Loadings. Transportation Research Record, 1896, 107–118.

Mandal, T., Edil, T. B., & Tinjum, J. M. (2018). Study on flexural strength, modulus, and fatigue cracking of cementitiously stabilised materials. Road Materials and Pavement Design, 19(7), 1546–1562.

Mandal, T., Tinjum, J. M., Gokce, A., & Edil, T. B. (2016). Protocol for Testing Flexural Strength, Flexural Modulus, and Fatigue Failure of Cementitiously Stabilized Materials Using Third-Point Flexural Beam Tests. Geotechnical Testing Journal, 39(1), 91–105.

Mbaraga, N. A., Jenkins, K. J., & van de Ven, M. (2014). Influence of Beam Geometry and Aggregate Size on the Flexural Strength and Elastic Moduli of Cement-Stabilized Materials. Transportation Research Record, 2401, 22–29.

Mgangira, M. B. (2011). Effect of method of curing on the flexural characteristics of a cement stabilised material. Proceedings of the 30th Southern African Transport Conference (SATC 2011), Pretoria.

Nascimento, R. S., & Albuquerque, F. S. (2018). Estudo de desempenho à fadiga de base cimentada tipo BGTC na BR-101/SE [Study of the fatigue performance of a cement-treated graded crushed stone base layer in BR-101/SE]. Transportes, 26(1), 21–36.

National Cooperative Highway Research Program (NCHRP). (2014). Characterization of Cementitiously Stabilized Layers for Use in Pavement Design and Analysis, Report 789. Washington DC, USA.

Otte, E. (1972). Die spanningsvervormingseienskappe van sementgestabiliseerde materiale [The stress-strain properties of cement-treated materials] (Master's thesis). University of Pretoria, South Africa.

Otte, E. (1978). A structural design procedure for cement-treated layers in pavements (Doctoral dissertation). University of Pretoria, South Africa.

Paige-Green, P. (2014). Cementitious stabilization of road materials, Council for Scientific and Industrial Research (CSIR) Report. Pretoria, South Africa.

Paiva, C. E. L., Oliveira, P. C. A., & Peixoto C. F. (2017). The influence of milling asphalt rates from wearing surface to the flexural strength applied to a recycled layer with Portland cement. Construction and Building Materials, 154, 1294–1300.

Paul, D. K., & Gnanendran, C. T. (2012). Characterisation of Lightly Stabilised Granular Base Materials by Flexural Beam Testing and Effects of Loading Rate. Geotechnical Testing Journal, 35(5).

Paul, D. K., & Gnanendran, C. T. (2015). Characterization of Lightly Stabilized Granular Base Materials Using Monotonic and Cyclic Load Flexural Testing. Journal of Materials in Civil Engineering, 28(1).

Paul, D. K., Theivakularatnam, M., & Gnanendran, C. T. (2015). Damage Study of a Lightly Stabilised Granular Material Using Flexural Testing. Indian Geotechnical Journal, 45(4), 441–448.

Pretorius, C. P. (1970). Design considerations for pavements containing soil cement bases (PhD thesis). University of California, Berkeley, California.

Robroch, S. (2002). Laboratory testing on foamed bitumen and cement treated material from the HVS test sections on road P243/1, Council for Scientific and Industrial Research (CSIR) Confidential Contract Report CR-2001/69. Pretoria, South Africa.

Sounthararajah, A., Bui, H. H., Nguyen, N., Jitsangiam, P., & Kodikara, J. (2018). Early-Age Fatigue Damage Assessment of Cement-Treated Bases under Repetitive Heavy Traffic Loading. Journal of Materials in Civil Engineering, 30(6).

Sounthararajah, A., Wong, L., Nguyen, N., Bui, H. H., & Kodikara, J. (2017). Evaluation of flexural behaviour of cemented pavement material beams using distributed fibre optic sensors. Construction and Building Materials, 156, 965–975.

Sounthararajah, A., Wong, L., Nguyen, N., Bui, H. H., Kodikara, J., & Jitsangiam, P. (2016). Flexural Properties of Cemented Granular Materials for Pavement Design. In: Chabot, A., Buttlar, W., Dave, E., Petit, C., & Tebaldi G. (eds) 8th RILEM International Conference on Mechanisms of Cracking and Debonding in Pavements. RILEM Bookseries, 13, 403–409. Springer, Dordrecht.

South African National Roads Agency Limited (SANRAL). (2014). South African Pavement Engineering Manual. Pretoria, South Africa.

Theyse, H. L. (2013). Construction of the stabilised base layer sections on the R104 experimental site: 1st Draft Version, Restricted Draft Contract Report SANRAL/SAPDM/D-3/2013-02. South Africa.

Theyse, H. L., De Beer, M., & Rust, F. C. (1996). Overview of South African mechanistic pavement design method. Transportation Research Record, 1539, 6–17.

Tokyay, M., & Özdemir, M. (1997). Specimen shape and size effect on the compressive strength of higher strength concrete. Cement and Concrete Research, 27(8), 1281–1289.

Trichês, G. (1993). Concreto compactado a rolo para aplicação em pavimentação: Estudo do comportamento na fadiga e proposição de metodologia de dimensionamento [Roller compacted concrete for pavements: Study on the fatigue behaviour and proposal of a structural design method] (Doctoral thesis). Brazilian Aeronautics Institute of Technology, Brazil.

Van Schalkwyk, F., & Kearsley, E. (2018). The influence of concrete compressive strength and specimen size on the compression stress block parameters of reinforced concrete. Journal of the South African Institution of Civil Engineering, 60(4), 34–44.

Washington State Department of Transportation (WSDOT). (2005). EVERSERIES USER'S GUIDE: Pavement Analysis Computer Software and Case Studies, Washington, DC.

Xiao, J., Jiang, W., Yuan, D., Sha, A., & Huang, Y. (2017). Effect of styrene–butadiene rubber latex on the properties of modified porous cement-stabilised aggregate. Road Materials and Pavement Design, 19(7), 1702–1715.

Yi, S. T., Yang, E. I., & Choi, J. C. (2006). Effect of specimen sizes, specimen shapes, and placement directions on compressive strength of concrete. Nuclear Engineering and Design, 236, 115–127.

Table 1. Characteristics of the natural gravels

Material	Weathered granite	Burnt shale
Liquid Limit, LL	28	25
Plasticity Index, PI	7	9
Linear Shrinkage (%)	3.5	6.5
Grading modulus, GM	2.27	2.46
HRB classification	A-2-4(0)	A-2-4(0)
TRH 14 classification*	G6	G6
Optimum moisture content, OMC (%)**	7.4	6.6
Maximum dry density, MDD (kg/m³)**	2106	2202
Swell (%)**	0.29	0.19
California Bearing Ratio, CBR (%)**	78	58

*Committee of State Road Authorities, CSRA, 1985; **Modified AASHTO compaction (American Association of State Highway and Transportation Officials, AASHTO, 2010); Shale results by Theyse (2013)

Table 2. Final mix design characteristics of the LCSM

Material	Weathered granite	Burnt shale
Initial consumption of stabilizer (%)	1.5	1.0
Lime content (%)	0.0	1.0
Cement content (%)	2.5	3.0
Unconfined compressive strength (MPa)	3.82*	3.21**
Indirect tensile strength (MPa)	0.42*	0.27**

*Accelerated curing, which successfully predicts the 7-day strength (CSRA, 1986; Paige-Green, 2014); **7 days; Shale results by Theyse (2013)

Table 3. Detailed programme for the static tests

Evaluated effect	Independent variable levels			Material (age)
	Compaction method	Test setup (mm × mm × mm)	Displacement rate (mm/min)	
Compaction method	Vibratory table Press Hammer	100 × 100 × 300	0.5	Granite (28 d)
Test setup (mm × mm × mm)	Vibratory table	100 × 100 × 300 75 × 75 × 420	0.5	Granite (28 d) Shale (28 d) Shale (5.5 y)
Displacement rate (mm/min)	Vibratory table	75 × 75 × 420	0.5 1.0 1.8	Granite (28 d)

Table 4. Statistical analysis of the compaction method effect on the static properties

Property	p-value	Compaction method	N	Mean	Grouping
MOR (MPa)	0.047	Vibratory table	3	0.507	A
		Press	3	0.445	A and B
		Hammer	3	0.354	B
UCS (MPa)	0.002	Vibratory table	3	3.512	A
		Press	3	2.495	B
		Hammer	3	1.918	B
Strain at break (με)	0.606	Vibratory table	3	309.6	A
		Press	3	282.5	A
		Hammer	3	249.7	A
Modulus (MPa)	0.529	Vibratory table	3	4043	A
		Press	3	3680	A
		Hammer	3	3381	A

Table 5. Statistical analysis of the test setup effect on the static properties

Material	Property	p-value	Test setup (mm × mm × mm)	N	Mean	Grouping
Granite 28 d	MOR (MPa)	0.002	100 × 100 × 300	3	0.51	A
			75 × 75 × 420	3	0.23	B
	UCS (MPa)	0.37	100 × 100 × 300	3	3.51	A
			75 × 75 × 420	3	3.27	A
	Strain at break (με)	0.684	100 × 100 × 300	3	269	A
			75 × 75 × 420	3	250	A
	Modulus (MPa)	0.011	100 × 100 × 300	3	4043	A
			75 × 75 × 420	3	2071	B
Shale 28 d	MOR (MPa)	0.012	100 × 100 × 300	3	0.89	A
			75 × 75 × 420	3	0.44	B
	UCS (MPa)	0.719	100 × 100 × 300	3	5.73	A
			75 × 75 × 420	3	5.53	A
	Strain at break (με)	0.085	100 × 100 × 300	3	395	A
			75 × 75 × 420	3	314	A
	Modulus (MPa)	0.005	100 × 100 × 300	3	4949	A
			75 × 75 × 420	3	2908	B
Shale 5.5 y	MOR (MPa)	0.034	100 × 100 × 300	3	1.13	A
			75 × 75 × 420	3	0.71	B
	UCS (MPa)	0.675	100 × 100 × 300	3	8.36	A
			75 × 75 × 420	3	8.76	A
	Strain at break (με)	0.102	100 × 100 × 300	3	673	A
			75 × 75 × 420	3	498	A
	Modulus (MPa)	0.009	100 × 100 × 300	3	6494	A
			75 × 75 × 420	3	3350	B

Table 6. Statistical analysis of the displacement rate effect on the static properties

Property	p-value	Displacement rate (mm/min)	N	Mean	Grouping
MOR (MPa)	0.289	0.5	3	0.23	A
		1	3	0.24	A
		1.8	3	0.32	A
UCS (MPa)	0.285	0.5	3	3.27	A
		1	3	3.93	A
		1.8	3	3.99	A
Strain at break (με)	0.332	0.5	3	269	A
		1	3	242	A
		1.8	3	199	A
Modulus (MPa)	0.283	0.5	3	2071	A
		1	3	2666	A
		1.8	3	3237	A

Table 7. Summary of cyclic tests results

Material	Stress level, SL (%)	Stress, σ_i (MPa)	Initial strain, ε_i (με)	Strain level (%)	Initial Modulus, M_i (MPa)	Number of cycles, N	UCS (MPa)
Granite 28 d	70	0.36	58	23	5432	40260	3.77
			63	25	5130	154102	3.59
	80	0.41	133	53	2883	12	3.91
			103	41	3551	419	4.03
	90	0.46	133	53	3222	1493	3.74
			68	27	6402	30408	4.06
Shale 28 d	70	0.62	75	19	5806	146435	5.83
	80	0.71	137	35	4799	297	6.40
	90	0.80	158	40	4772	131	6.89

Table 8. Fatigue lives predicted for the cement stabilized shale layer

Tire pressure (kPa)	LCSM parameters	Fatigue model	Number of load repetitions, N
560	This study (Modulus = 1331 MPa; Strain at break = 395 με)	Laboratory	1
		TF RL = 50%	2061281
		TF RL = 80%	1334320
		TF RL = 90%	1246226
		TF RL = 95%	944031
	South African mechanistic pavement design method (Modulus = 2000 MPa; Strain at break = 125 με)	Laboratory	1
		TF RL = 50%	96232
		TF RL = 80%	62581
		TF RL = 90%	58530
		TF RL = 95%	44226
800	This study (Modulus = 1331 MPa; Strain at break = 395 με)	Laboratory	1
		TF RL = 50%	1406492
		TF RL = 80%	910982
		TF RL = 90%	850984
		TF RL = 95%	644430
	South African mechanistic pavement design method (Modulus = 2000 MPa; Strain at break = 125 με)	Laboratory	1
		TF RL = 50%	38099
		TF RL = 80%	24811
		TF RL = 90%	23215
		TF RL = 95%	17528

Table 9. Statistical analysis of South African and Brazilian LCSM flexural properties

Property	p-value	Country	Material	N	Mean	Grouping
MOR (MPa)	0.000	South Africa	Granite	3	0.51	B
			Shale	3	0.89	A
		Brazil	20% RAP	3	0.26	C
			50% RAP	3	0.32	B and C
Static modulus (MPa)	0.005	South Africa	Granite	3	4043	A and B
			Shale	3	4949	A
		Brazil	20% RAP	3	3950	A and B
			50% RAP	3	2900	B
Strain at break (με)	0.012	South Africa	Granite	3	250	A and B
			Shale	3	395	A and B
		Brazil	20% RAP	3	169	B
			50% RAP	3	470	A

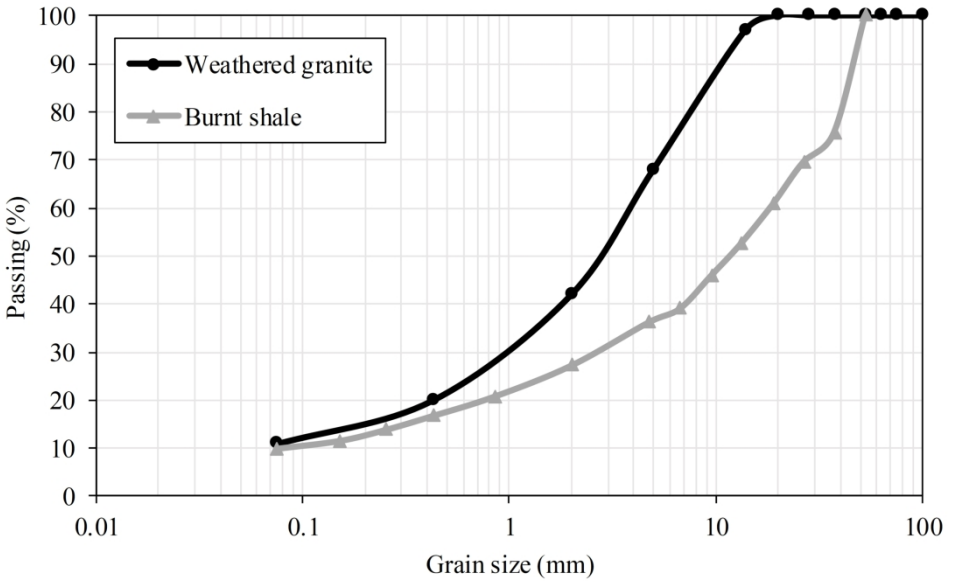

137x85mm (600 x 600 DPI)

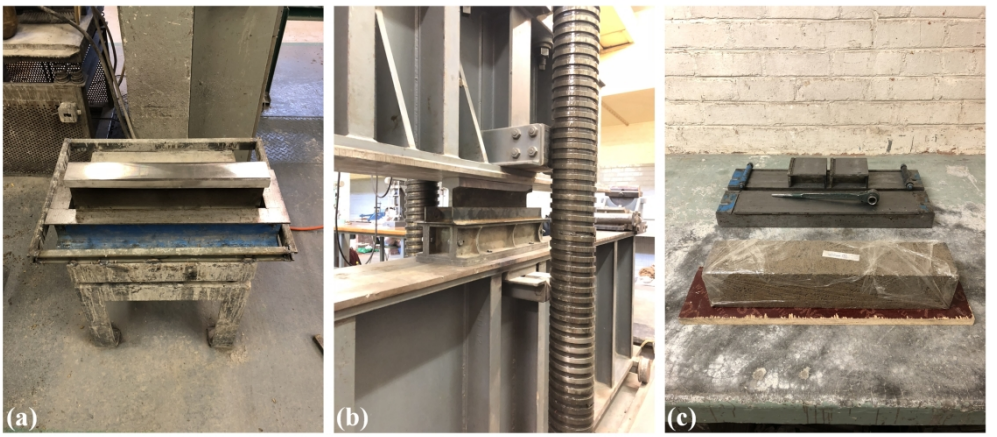

149x66mm (600 x 600 DPI)

100x66mm (600 x 600 DPI)

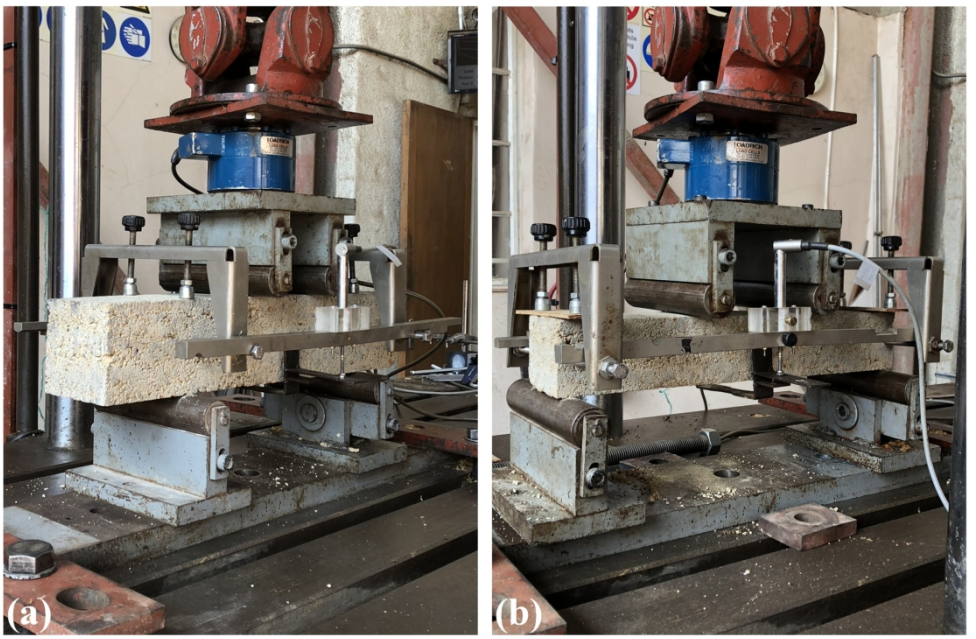

100x66mm (600 x 600 DPI)

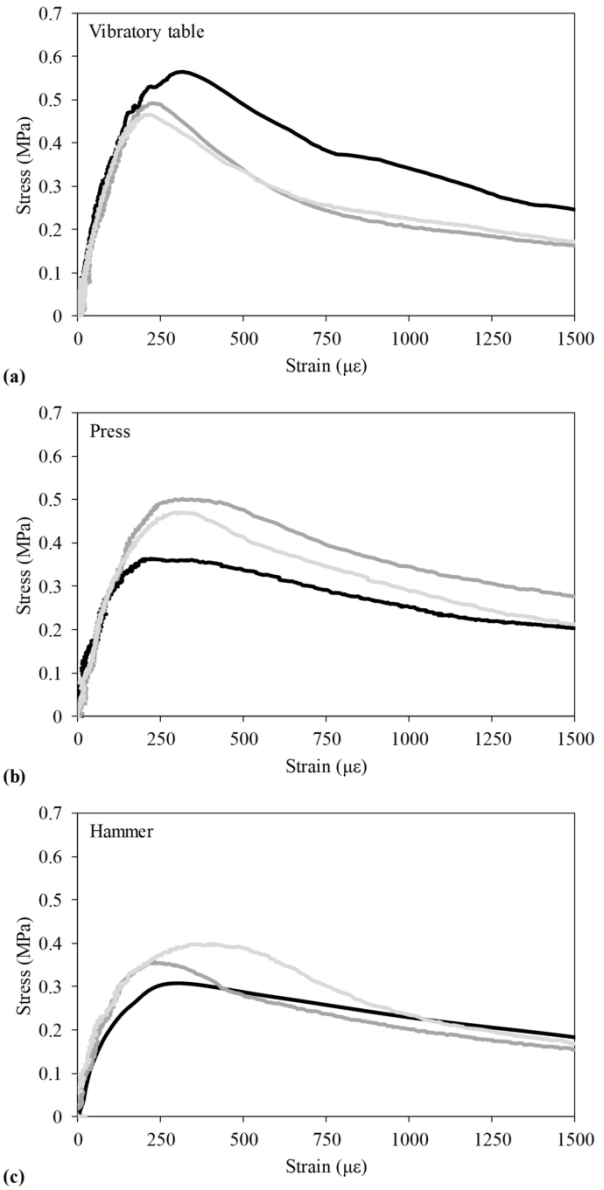

58x108mm (600 x 600 DPI)

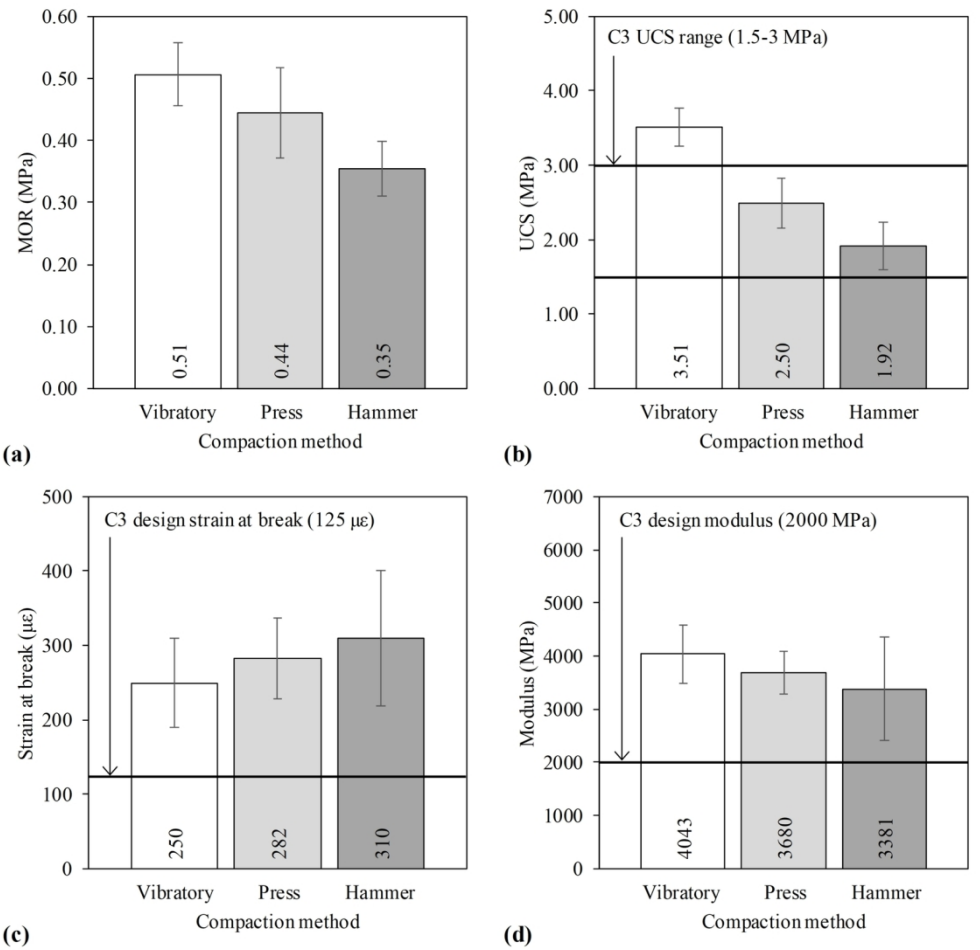

75x72mm (600 x 600 DPI)

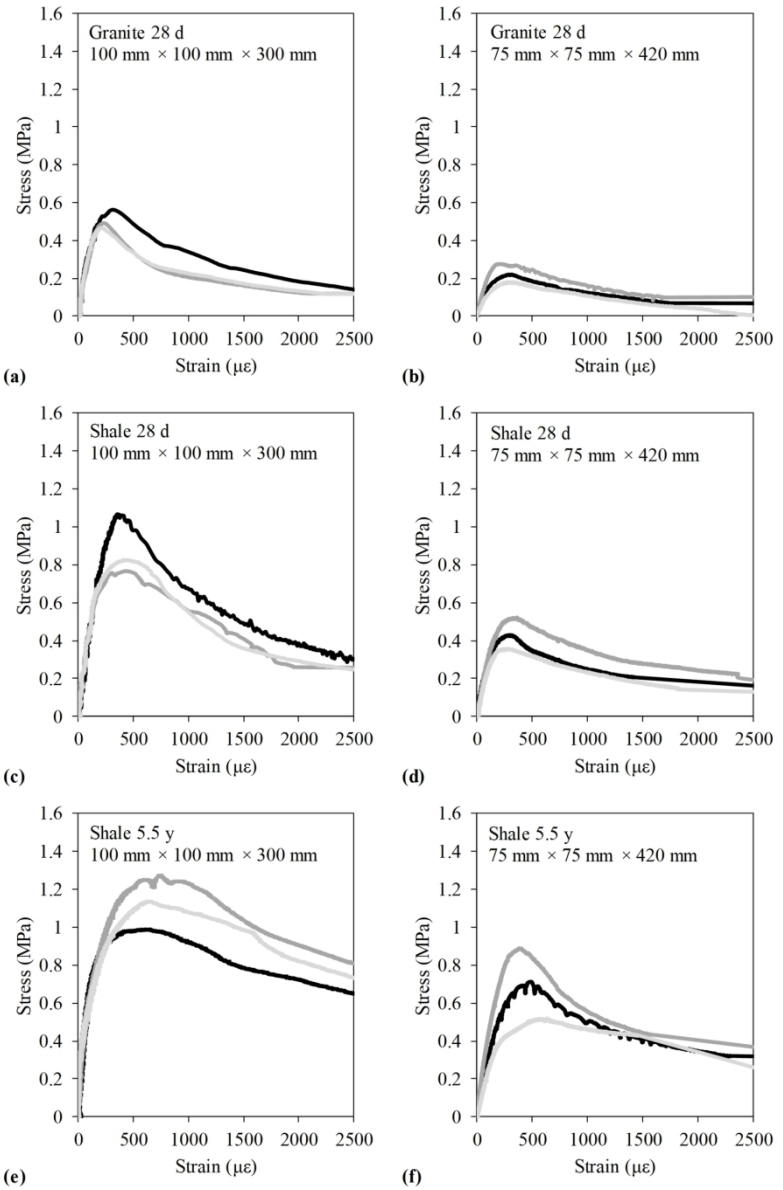

74x106mm (600 x 600 DPI)

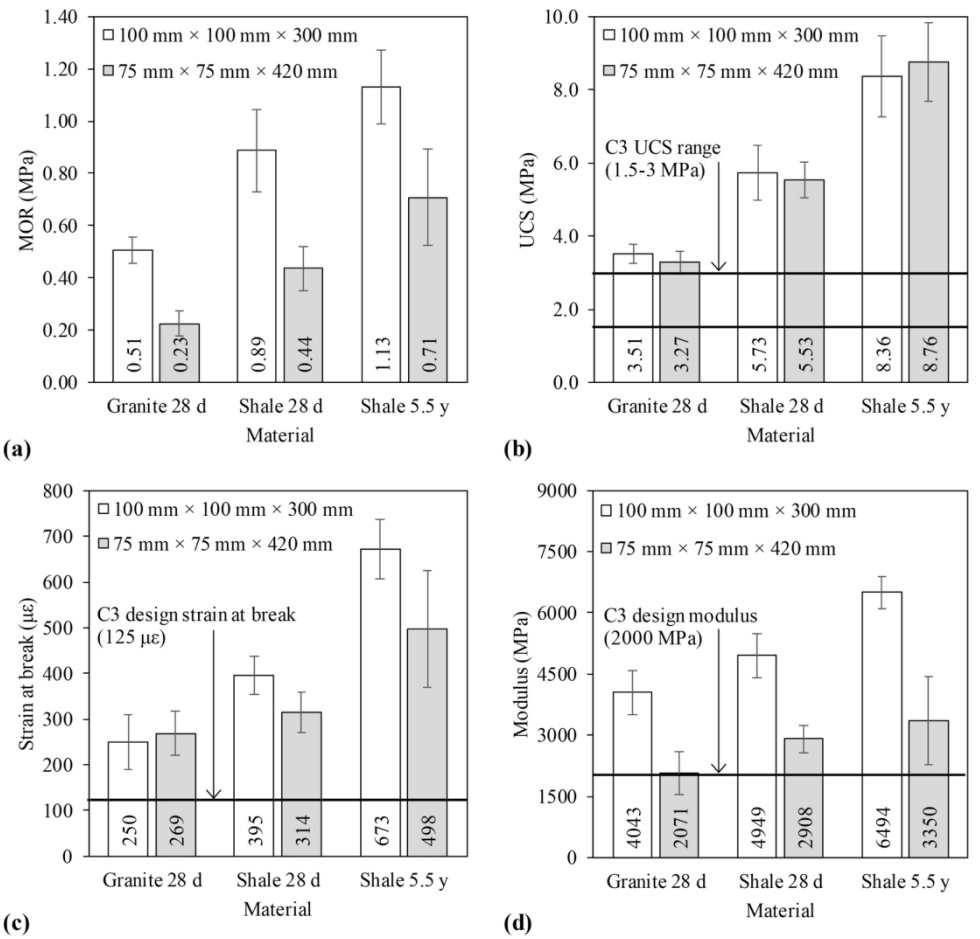

74x71mm (600 x 600 DPI)

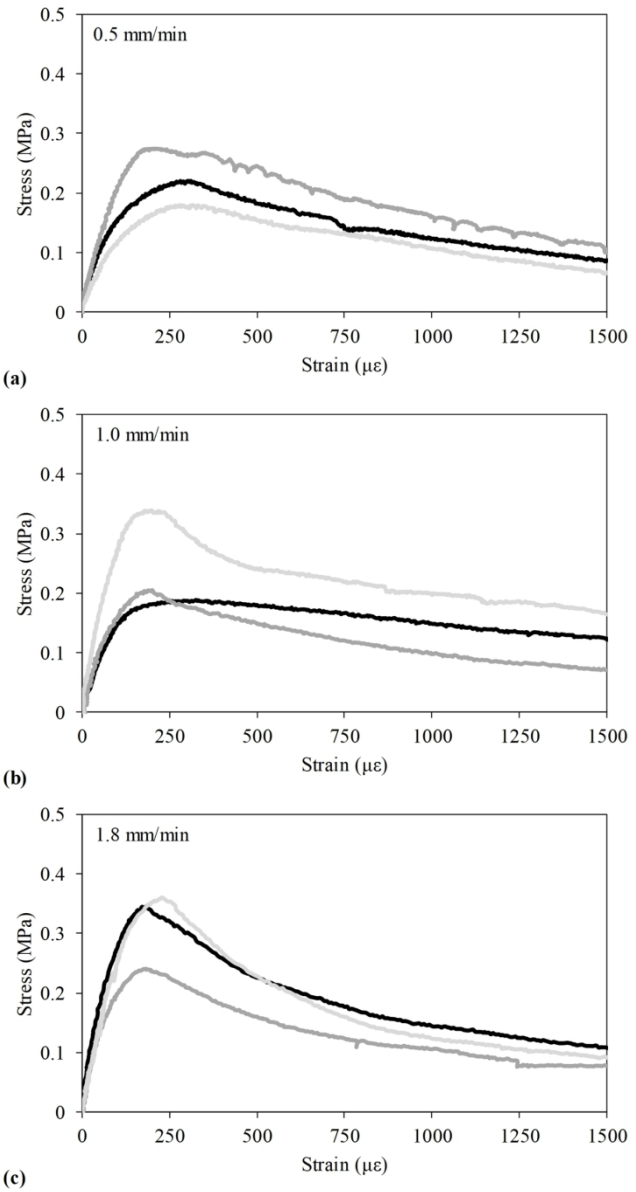

58x105mm (600 x 600 DPI)

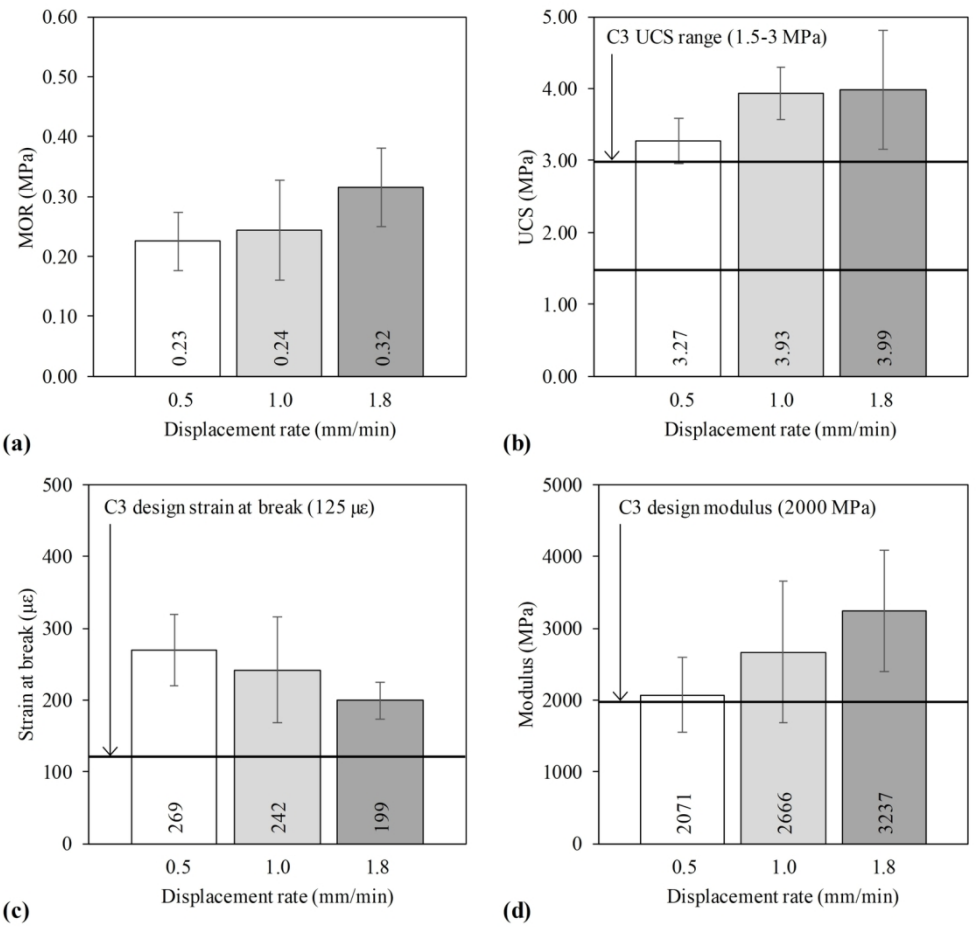

75x70mm (600 x 600 DPI)

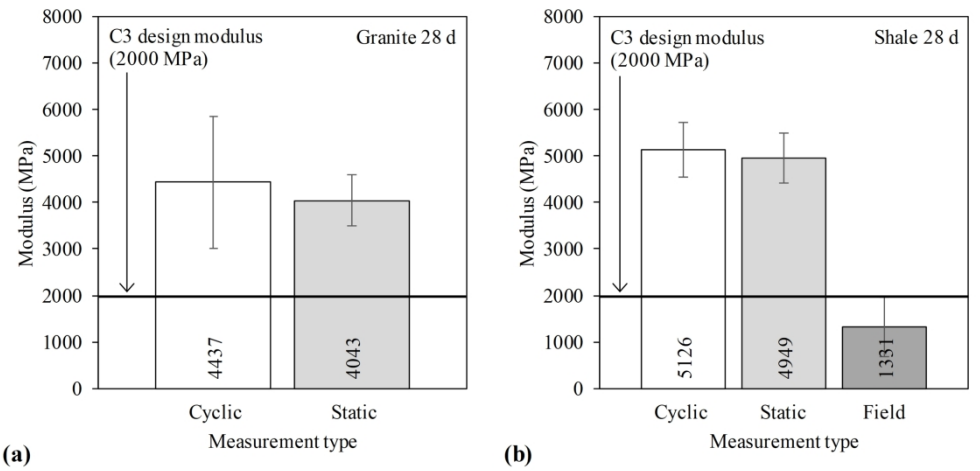

149x72mm (600 x 600 DPI)

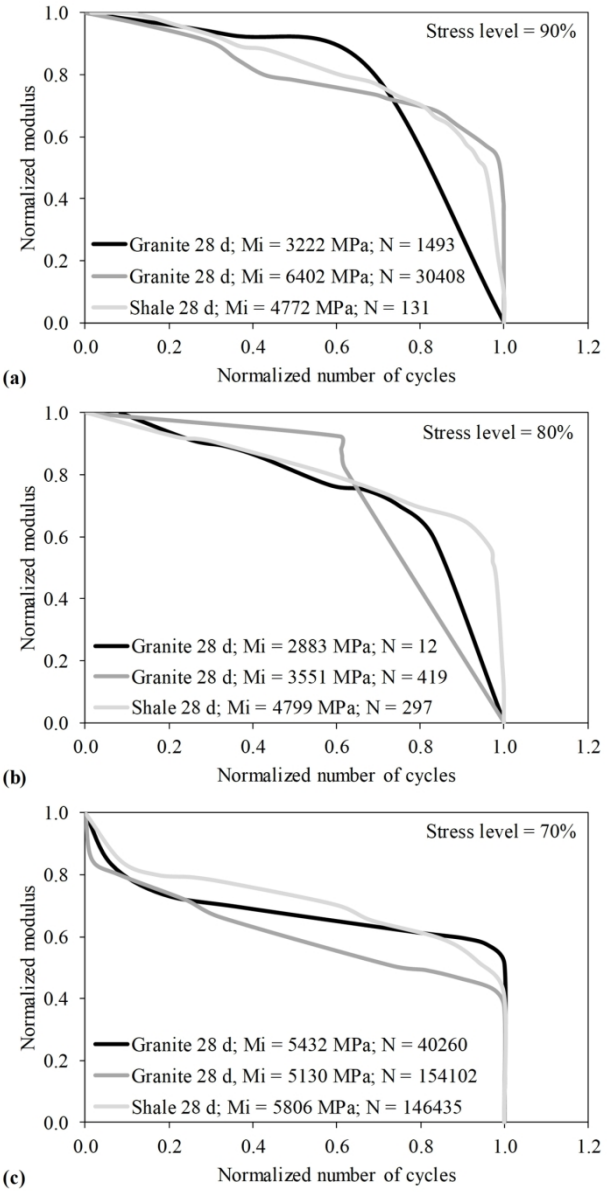

58x106mm (600 x 600 DPI)

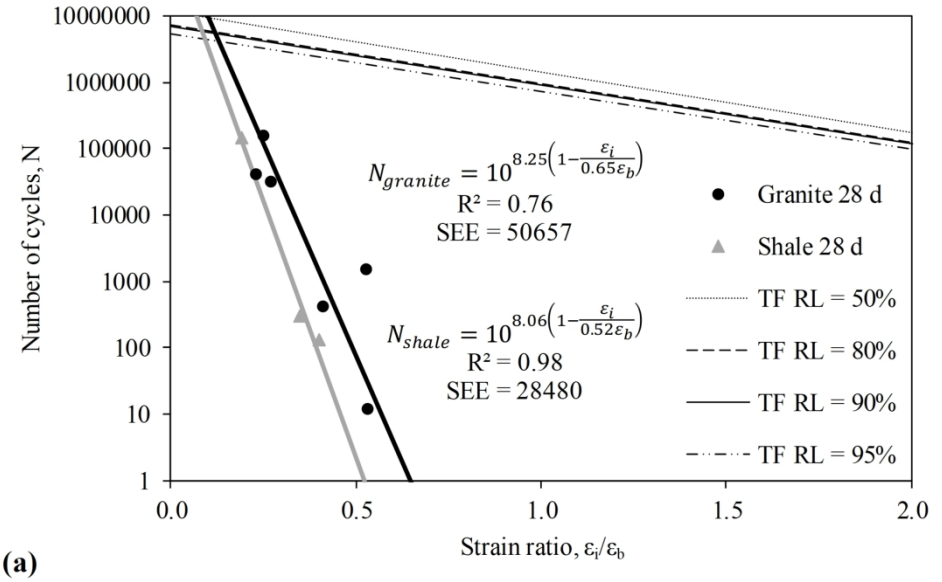

(a)

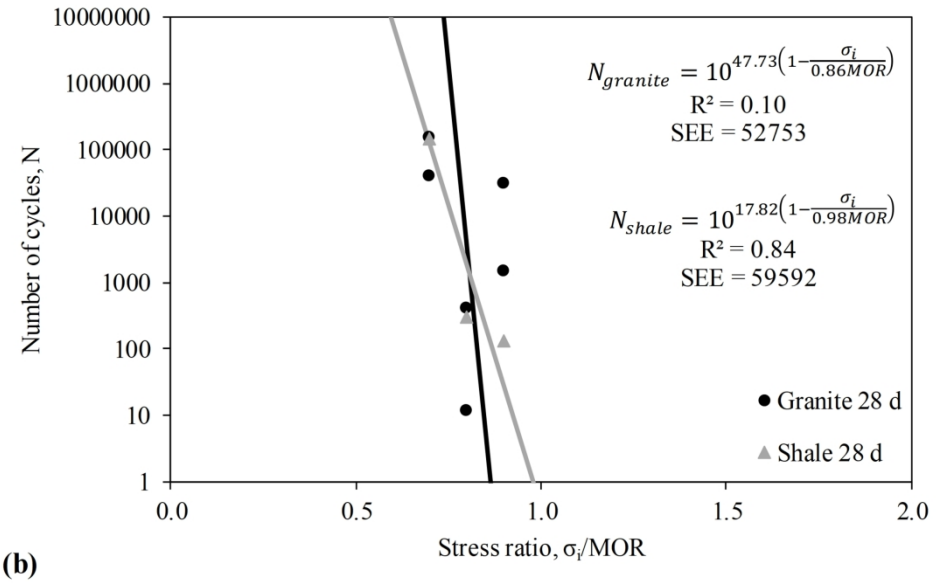

(b)

116x144mm (600 x 600 DPI)

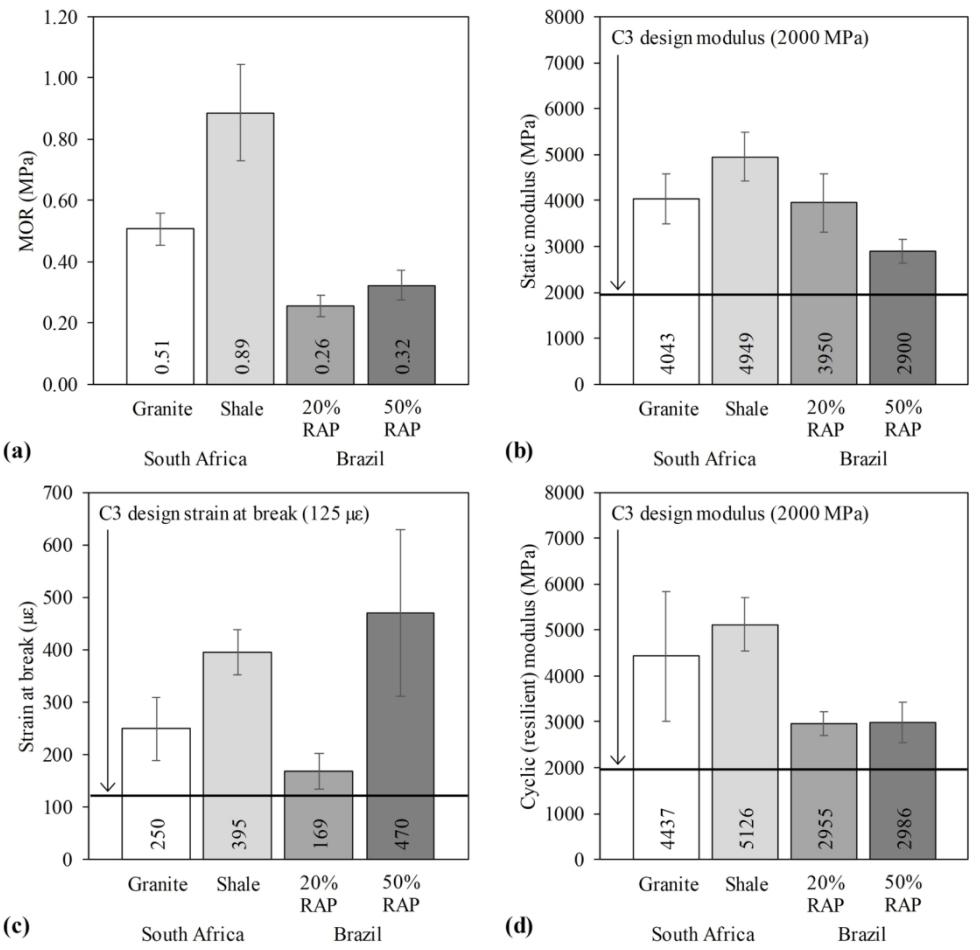

75x71mm (600 x 600 DPI)

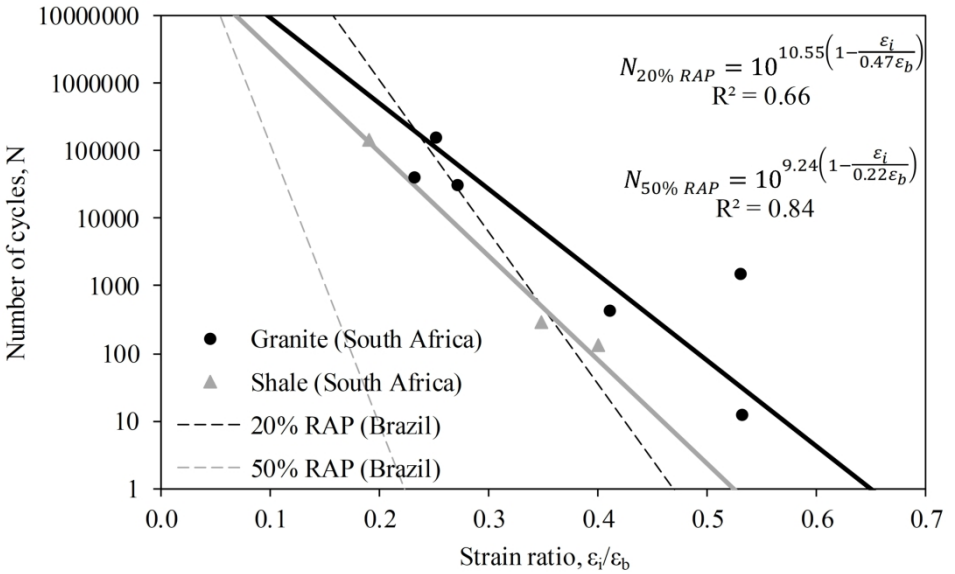

137x85mm (600 x 600 DPI)